Characterisation of the ACE-FTS instrument line shape

Robert Poulin*, Yvan Dutil, Stéphane Lantagne, and François Châteauneuf
ABB Advanced Analytical Solutions, 585 Charest Blvd East, Suite 300, Québec, G1K 9H4, Canada

ABSTRACT

The Atmospheric Chemistry Experiment (ACE) is the mission selected by the Canadian Space Agency for its new science satellite, SCISAT-1. Dr. Peter Bernath of the University of Waterloo is the ACE Mission Scientist, and ABB is the industrial contractor for the development of the ACE primary instrument. The ACE primary instrument is an infrared Fourier Transform Spectrometer (FTS) coupled with an auxiliary 2-channel visible and near infrared imager. The FTS, operating from 2.4 to 13.3 microns, will measure at an unapodised resolution of 0.02 cm-1 the infrared absorption signals that contain information on different atmospheric layers to provide vertical profiles of atmospheric constituents. Its highly folded design results in a very high performance instrument with a compact size. The imager will monitor aerosols based on the extinction of solar radiation using two filtered detectors at 1.02 and 0.525 microns. The instrument also includes a suntracker, which provides the sun radiance to both the FTS and the imager during solar occultation of the earth's atmosphere. In order to meet all science objectives, the instrument line width of the ACE-FTS has to be smaller than 0.028 cm–1. There are however different instrument function contributors affecting the width and the symmetry of spectral lines. These contributors are related to effects inherent to the instrument. This paper will describe these different effects and their impacts on the instrument line shape (ILS). Results obtained during the ILS characterisation of the flight model will be presented. A short description of a correction algorithm is also discussed.

Keywords: ACE, Infrared, Spectrometer, Fourier, ILS, Shape

1. INTRODUCTION

The impulse response of a Fourier transform spectrometer is affected by different instrument function contributors which are due to effects inherent to the instrument. Starting from an elementary line contribution, e.g., emission from a single gas molecule, interactions between the molecules, expressed as temperature and pressure, produce a line broadening (C0 in Fig. 1).

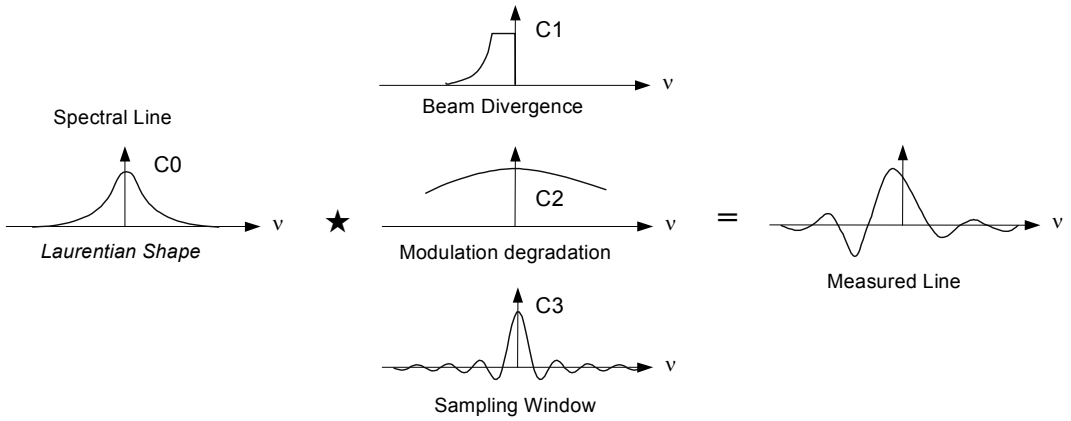

Figure 1: Instrument function contributors

This physical effect cannot be removed and reflects in fact some of the gas properties which we want to measure. The first instrument contribution illustrated here (C1) is due to self-apodisation. As the emitted energy enters the interferometer, different angles for the different fields of view produce different apparent spectral frequencies. A monochromatic signal thus produces a continuum of frequencies. The shape of this continuum is a function of the pixel

* robert.h.poulin@ca.abb.com; phone (418) 877-2944 x451

Proceedings of SPIE Vol. 5151 Earth Observing Systems VIII, edited by William L. Barnes
(SPIE, Bellingham, WA, 2003) · 0277-786X/2003/$15.00

geometry, the pixel position with respect to the optical axis, and the spectral frequency of the signal. The corresponding line shape is indicated by Beam Divergence in Fig. 1. The second effect (C2) is due to perturbations like shear and tilt on the interfering beam which may fluctuate causing distortions on the measured lines. The corresponding line shape is indicated by Modulation Degradation in Fig. 1. The third contribution (C3) is due to acquisition of interferograms which are of finite length. This third effect introduces the Sinc "dressing". The corresponding line shape is indicated by Sampling Window in Fig. 1. The mathematical operation for applying the contributions C2 and C3 to the gas line is expressed either by multiplication when considering the interferogram domain or by convolution when considering the spectral domain. However, the first contribution C1, i.e. self-apodisation, can not be treated as a simple convolution in either domain since this effect is non-local in both domains.

A good understanding of the FTS transfer function is very important when considering radiometric calibration or retrieval of atmospheric properties. In fact, when applying the two-point radiometric calibration, the instrument gain and offset are retrieved from measurement of the radiance from known sources. For radiometric measurements, this known radiance is modelled as the Planck radiation function at the temperature of the source multiplied by the effective emissivity of the source. For instruments working in solar occultation like the ACE-FTS, the reference measurements are the exo-atmospheric spectrum of the Sun and the spectrum of the deep space to calibrate out the offset. Since there are spectral features in the Solar spectrum, the retrieval of the instrument gain is not straightforward. Lines in the references spectrum are spread out over a spectral extent that may contain atmospheric features targeted for the retrieval.

2. INSTRUMENT LINE SHAPE MODELLING

The effects of the instrument line shape (ILS) on the signal can be seen as the action of a given operator $\hat{A}$ on the signal vector, $|L\rangle$, i.e.

$$|L'\rangle = \hat{A}|L\rangle \tag{1}$$

Since the instrument line shape operator is not local in the spectrum representation or in the interferogram representation we choose to represent its action as a Fredholm integral equation of the first kind,

$$|L'\rangle = \int d\nu \int d\nu' \, |\nu\rangle\langle\nu|\hat{A}|\nu'\rangle\langle\nu'|L\rangle \tag{2}$$

or

$$L(\nu) = \int A(\nu;\nu') L(\nu') \, d\nu' \tag{3}$$

where A may now be seen as the instrument response to an impulse at ν'. This operator can take many forms to model different effects. Three of these effects are listed below.

2.1 Off-Axis Effects

The operator $\hat{A}$ can include many effects and one of them is the self-apodisation [1,2] (contributor C1 in Fig. 1).

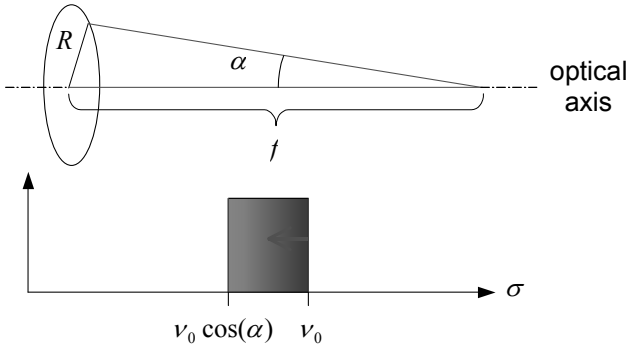

Figure 2: Off-axis effect and line broadening impact

To understand this self-apodisation effect, consider that every monochromatic component of light travelling in the effective direction produces an interference signal that oscillates with the frequency corresponding to the correct wavenumber. However, if the wave vector of the monochromatic plane wave component with wavenumber ν_0 makes an angle α with respect to the optical axis of the interferometer, its interference signal has a cosine dependence which oscillates at a frequency corresponding to the wavenumber $\nu_0 \cos(\alpha)$. This produces a broadening of the monochromatic lines as shown in Fig. 2.

2.2 Reference laser wavelength drift

In order to consider this effect, an operator $\hat{D}$ representing a shrink or a stretch of the spectral axis is introduced. This operator is not local in either representation and can be written in the spectrum representation as

$$\langle \nu' | \hat{D} | \nu \rangle = \frac{1}{1+d} \delta(\nu(1+d) - \nu'). \tag{4}$$

Within a small spectral region, this shrink or stretch can be seen as a shift of the spectral axis. In the interferogram representation, this drift can therefore be considered as a multiplication by a phase factor proportional to the shift in the spectral representation.

2.3 Fringe contrast variation over OPD

Since other effects may not be negligible, the correction of the off-axis effect may be not sufficient. For example, the modulation efficiency may vary with the optical path difference. Phenomenon like residual diffraction or mechanical imperfection may be responsible for this effect. In order to consider those effects, an operator $\hat{R}$ representing a modulation term over the interferogram is introduced. This operator is local in the interferogram representation, i.e.

$$\langle x' | \hat{R} | x \rangle = R(x)\, \delta(x - x') \tag{5}$$

and we choose to model this modulation term as a fourth order polynomial,

$$R(x) = c_0 + c_1 x + c_2 x^2 + c_3 x^3 + c_4 x^4. \tag{6}$$

3. INSTRUMENT LINE SHAPE CHARACTERISATION

The ILS characterisation flow chart is presented in Fig. 3. A different characterisation and modelling algorithm was presented in [3].

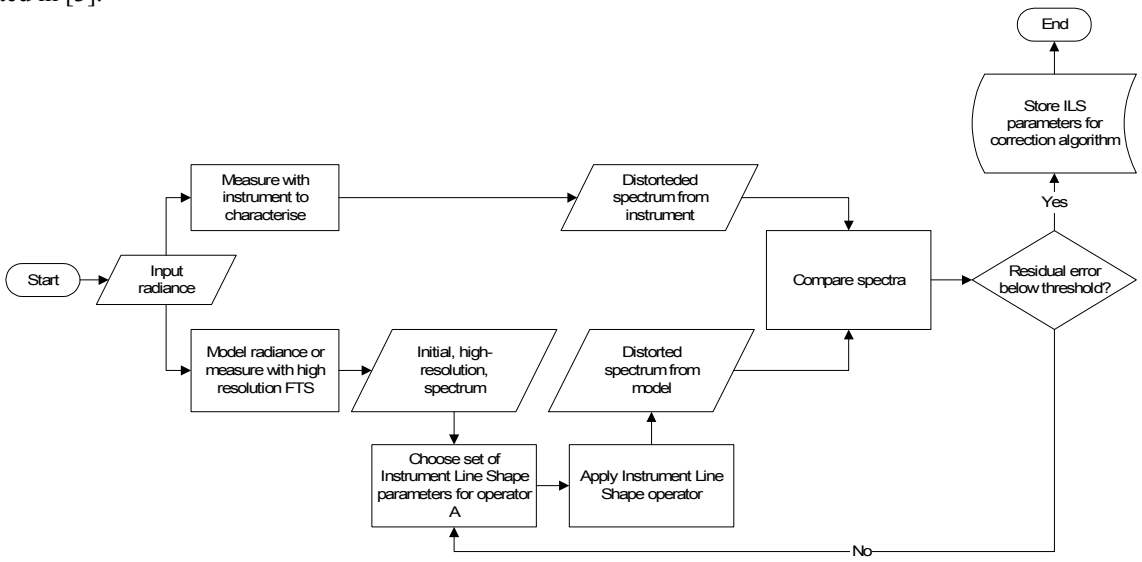

Figure 3: Instrument line shape characterisation flow diagram.

First, an input radiance with narrow absorption or emission lines is measured with the instrument to characterise. The distorted spectrum from the instrument is then obtained. To produce the reference spectrum, the same radiance can be either modelled or measured at high resolution so that absorption or emission lines are resolved to their natural shape. Once these two sets of data are obtained, the characterisation becomes an iterative optimisation process on the ILS parameters (e.g. maximum optical path difference, off-axis rays geometry, divergence, modulation variation vs. optical path difference, etc.). The initial guess for the ILS parameters may even come from a pre-characterisation of the instrument. Once the distorted spectrum is close to the measured spectrum up to a certain threshold value, the ILS parameters are stored in order to feed the correction algorithm.

Many cost functions can be used to determine the closeness of the simulated spectrum to the measured one. It could be the mean of the normalized square difference, i.e.

$$C^2 = \sum_k \{L_{meas}[k] - L_{sim}[k]\}^2 \tag{7}$$

where L_{meas} is the measured spectrum, L_{sim} is the simulated spectrum and $\langle L[k] \rangle$ represents the mean of the spectrum. It can also be the correlation coefficient between the two spectra, i.e.

$$R^2 = \frac{\left\{\sum_k L_{meas}[k] - L_{sim}[k]\right\}^2}{\left\{\sum_k L_{meas}[k] - \langle L_{meas}[k] \rangle\right\}^2 - \left\{\sum_k L_{sim}[k] - \langle L_{sim}[k] \rangle\right\}^2}. \tag{8}$$

The cost function is therefore parameterised by the same parameters that are used to represent the ILS operator.

3.1 Retrieval on Experimental Data

As a first example, the parameter space is explored using the N_2O absorption spectrum measured with the ACE-FTS instrument at a spectral sampling of 0.02 cm^{-1}. The measured and theoretical spectra are shown in Fig. 4. The gas cell was filled with 12 torr of gas and its temperature was 33 degrees Celsius.

The data were collected at the University of Toronto during the verification campaign of the flight unit of the ACE-FTS instrument[4]. Averaging of reference and gas spectra has been performed to obtain a signal-to-noise ratio of about 500 on the gas transmittance.

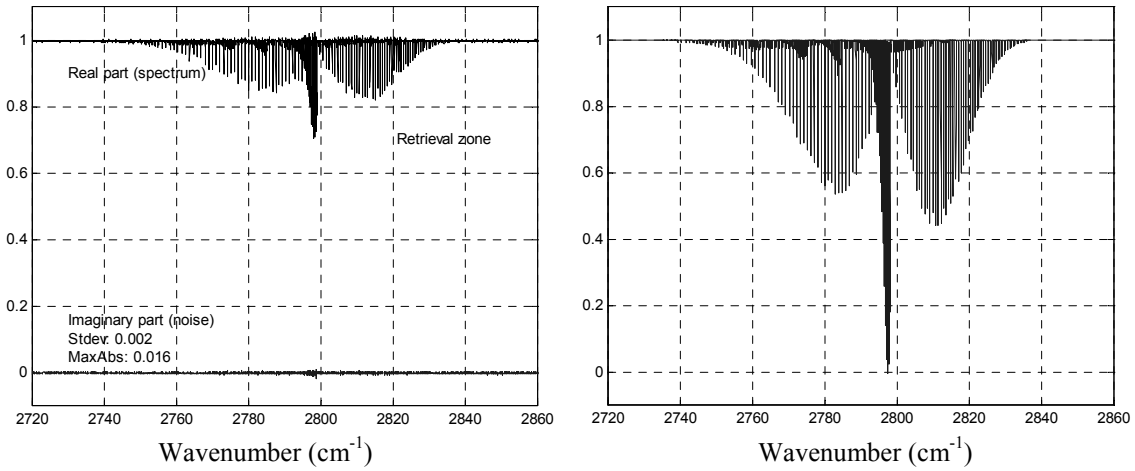

Figure 4: Measured (left) and theoretical (right) N_2O absorption spectra.

Using these data, a first retrieval of the laser reference wavelength is performed by stretching the spectral axis such that a good match is obtained between the measured spectrum and theoretical spectrum affected by the nominal ILS distortion. The nominal ILS distortion must be understood as the ILS produced with the parameter values defined by design. For the ACE-FTS instrument, the nominal distortion considers a sampling interval of 0.02 cm^{-1} and a circular divergence inside the interferometer of 3.125 mrad in radius centred on the optical axis. Note that the input telescope of the ACE-FTS instrument maps the instrument FOV of 1.25 mrad to the interferometer divergence with a magnification factor of 5. The measured and simulated spectra are shown in Fig. 5 and the cost using the mean of the normalised square difference is estimated at 3.285.

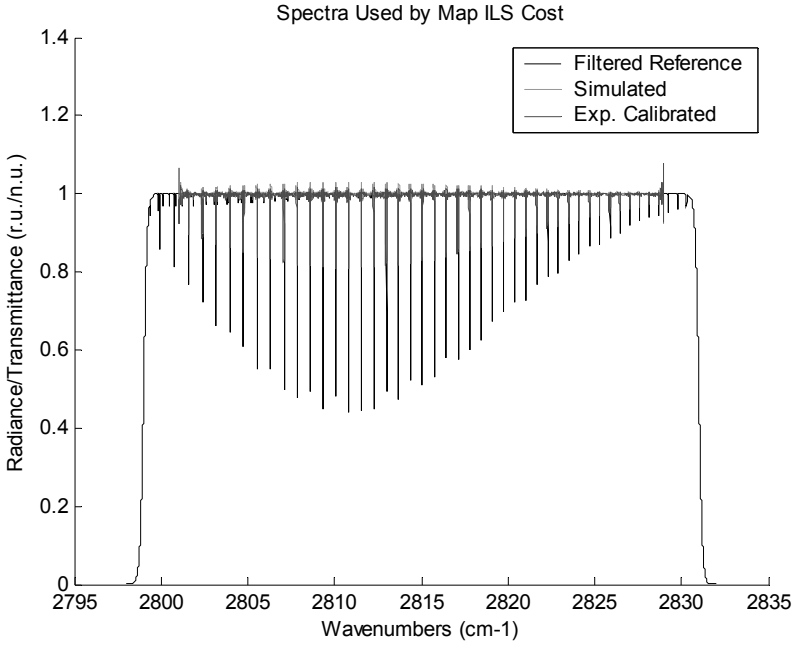

Figure 5: Simulated and experimental spectra for nominal ILS distortion. The cost value is 3.285.

Once the stretch factor is obtained, a series of simulated spectra is generated to cover a small portion of the ILS parameter space centred around the nominal configuration of the interferometer divergence. This mapping shown in Fig. 6 reveals a valley starting at coordinate [size: 3.5 mrad, position: 0 mrad] and going down to coordinate [size: 2 mrad, position: 2 mrad]. Along this valley, there are few local minima with a minimum minimorum at coordinate [size: 2.55 mrad, position: 1.28 mrad].

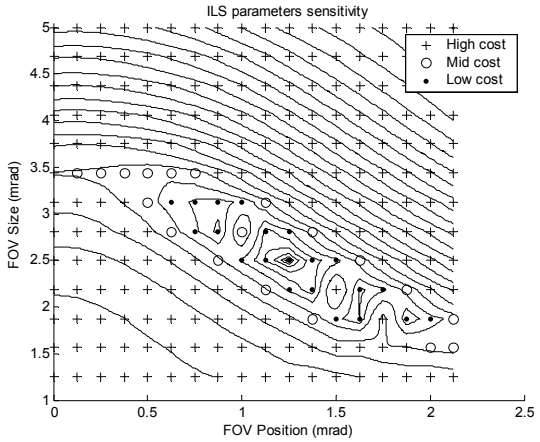

Figure 6: Mapping of the cost in a 2-dimension parameter space.

A measured absorption line along with a simulated line calculated with the retrieved parameters is shown in Fig. 7. The fit shows good agreement with local mismatch of the order of 1 %.

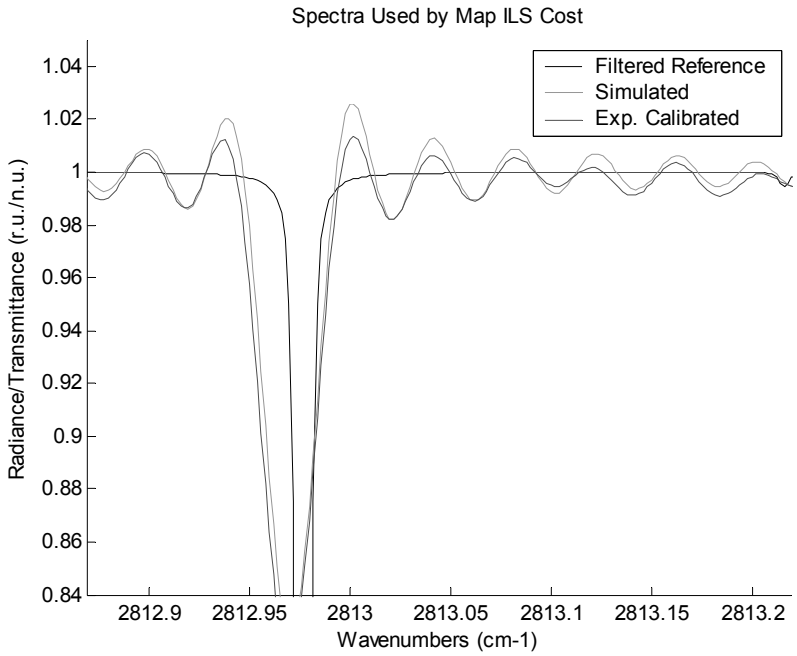

Figure 7: Measured and fitted N_2O absorption line for a half divergence inside the interferometer of 5.1 mrad offset from the optical axis by 1.28 mrad.

4. INSTRUMENT LINE SHAPE CORRECTION

The correction algorithm is derived to remove all ILS contributor except from contributors C0 and C3 of Fig. 1. In fact, C0 contains part of the information to be retrieved and C3 implies an a priori knowledge of the natural line shapes in the spectrum. The correction matrix is derived from Eq.1 by inserting the continuous identity operator twice and the discrete identity operator once, i.e.

$$\left|L'\right\rangle = \int d\nu \int d\nu' \sum_k \left|\nu\right\rangle\left\langle\nu\right|\hat{A}\left|\nu'\right\rangle\left\langle\nu'\right|\left|\nu_k^{MPD}\right\rangle\left\langle\nu_k^{MPD}\right|\left|L\right\rangle \tag{9}$$

where

$$\left\langle\nu'\middle|\nu_k^{MPD}\right\rangle = \mathrm{Sinc}\left(2MPD\left(\nu_k - \nu'\right)\right), \tag{10}$$

and projecting both sides on $\left|\nu_k^{MPD}\right\rangle$. The ILS application matrix is then obtained within the approximation that the function $A(\nu;\nu')$ is constant over the extent of the basis set function $\mathrm{Sinc}\left(2MPD(\nu_k - \nu')\right)$. Inversion of this matrix finally gives the ILS correction operator. Preliminary results from numerical simulations show that the correction algorithm brings the error below 0.1 % for a typical absorption spectrum.

5. CONCLUSIONS

Flexible ILS modelling tools have been developed and used to derive a flexible ILS retrieval algorithms implemented into a Matlab library of functions. ILS parameters have been retrieved on experimental taken with the ACE-FTS instrument during the verification campaign. The retrieved parameters suggest that the full divergence inside the interferometer is 5.1 mrad with an offset of 1.28 mrad from the optical axis. However, a more accurate theoretical

reference spectrum could improve the results (accurate gas cell pressure, temperature and length). Finally, an ILS correction scheme was described.

REFERENCES

1. P. Saarinen and J. Kauppinen, Appl. Opt., **31**, 2353-2359 (1992)
2. J. Genest and P. Tremblay, Appl. Opt., **38**, 5438-5446 (1999)
3. K. W. Bowman, H. M. Worden, and R. Beer, Appl. Opt., **39**, 3765-3773
4. K. Walker and C. Boone, Private communication